The EMBO Journal Vol. 21 No. 15 pp. 4070–4080, 2002

Sequential involvement of Cdk1, mTOR and p53 in apoptosis induced by the HIV-1 envelope

Maria Castedo, Thomas Roumier, Julià Blanco[1], Karine F.Ferri, Jordi Barretina[1], Lionel A.Tintignac, Karine Andreau, Jean-Luc Perfettini, Alessandra Amendola[2], Roberta Nardacci[2], Philip Leduc[3], Donald E.Ingber[3], Sabine Druillennec[4], Bernard Roques[4], Serge A.Leibovitch, Montserrat Vilella-Bach[5], Jie Chen[5], José A.Este[1], Nazanine Modjtahedi, Mauro Piacentini[2,6] and Guido Kroemer[7]

Centre National de la Recherche Scientifique, UMR1599, Institut Gustave Roussy, 39 rue Camille-Desmoulins, F-94805 Villejuif, [4]Unité de Pharmacochimie Moléculaire et Structurale, INSERM U266–CNRS UMR860, Université René Descartes (Paris V), F-75005 Paris, France, [1]Institut de Recerca de la SIDA-Caixa, Laboratori de Retrovirologia, Hospital Universitari Germans Trias i Pujol, Universitat Autónoma de Barcelona, Ctra Canyet s/n, 08916 Badalona, Catalonia, Spain, [2]Istituto Nazionale Malattie Infettive 'L. Spallanzani', Rome 00149, [6]Department of Biology, University of Rome Tor Vergata, Rome 00133, Italy, [3]Departments of Surgery and Pathology, Children's Hospital and Harvard Medical School, Enders 1007, 300 Longwood Avenue, Boston, MA 02115 and [5]Department of Cell and Structural Biology, University of Illinois at Urbana-Champaign, Urbana, IL 61801, USA

[7]Corresponding author
e-mail: kroemer@igr.fr

Syncytia arising from the fusion of cells expressing the HIV-1-encoded *Env* gene with cells expressing the CD4/CXCR4 complex undergo apoptosis following the nuclear translocation of mammalian target of rapamycin (mTOR), mTOR-mediated phosphorylation of p53 on Ser15 ($p53^{S15}$), p53-dependent upregulation of Bax and activation of the mitochondrial death pathway. $p53^{S15}$ phosphorylation is only detected in syncytia in which nuclear fusion (karyogamy) has occurred. Karyogamy is secondary to a transient upregulation of cyclin B and a mitotic prophase-like dismantling of the nuclear envelope. Inhibition of cyclin-dependent kinase-1 (Cdk1) prevents karyogamy, mTOR activation, $p53^{S15}$ phosphorylation and apoptosis. Neutralization of p53 fails to prevent karyogamy, yet suppresses apoptosis. Peripheral blood mononuclear cells from HIV-1-infected patients exhibit an increase in cyclin B and mTOR expression, correlating with $p53^{S15}$ phosphorylation and viral load. Cdk1 inhibition prevents the death of syncytia elicited by HIV-1 infection of primary CD4 lymphoblasts. Thus, HIV-1 elicits a pro-apoptotic signal transduction pathway relying on the sequential action of cyclin B–Cdk1, mTOR and p53.

Keywords: cell death/cyclin B/mitochondria/p53/rapamycin

Introduction

Fusion of somatic cells, resulting in the formation of syncytia, is a normal process involved in the generation of myotubes, osteoclasts and the syncytiotrophoblast (Anderson, 2000). In contrast, non-physiological heterokaryon formation ultimately results in cell death, as this has been shown by overexpression of fusogenic viral glycoproteins, thereby enforcing syncytium formation (Bateman *et al*., 2000; Scheller and Jassoy, 2001). This applies also to the fusion of cells expressing Env, the envelope glycoprotein complex (gp120/gp41) encoded by the HIV type 1 (HIV-1) genome, with cells expressing the Env (co-)receptor, a combination of CD4 with either CXCR4 or CCR5. Syncytium formation resulting from the Env–CD4 interaction leads to apoptosis, a process thought to participate in the AIDS-associated depletion of $CD4^+$ T lymphocytes (Lifson *et al*., 1986; Sodroski *et al*., 1986; Blaak *et al*., 2000; Maas *et al*., 2000; Mohri *et al*., 2001). Indeed, it appears that Env is (one of) the functionally most important apoptogenic HIV-1 product(s) (Gougeon and Montagnier, 1999; Badley *et al*., 2000; Selliah and Finkel, 2001). The Env complex is expressed on the surface of HIV-1-infected cells as well as on HIV-1 virions. Within this complex, gp120 mediates the primary interaction with the receptor/co-receptor complex, while gp41 participates in membrane interactions eventually leading to fusion (Eckert and Kim, 2001). The interaction between Env and the co-receptor can also mediate pro-apoptotic signals, the exact nature of which is a matter of debate. Env-elicited apoptosis may involve caspases, caspase-independent effectors, inactivation of survival signals mediated by focal adhesion complexes and calcineurin activation, as well as mitochondrial membrane permeabilization (Berndt *et al*., 1998; Cicala *et al*., 2000; Roggero *et al*., 2001; Vlahakis *et al*., 2001; Sasaki *et al*., 2002).

Syncytial apoptosis induced by the Env–CD4 interaction involves a precise sequence of events: (i) activation of the mammalian target of rapamycin (mTOR), a serine/threonine kinase of the phosphatidyl inositol kinase family; (ii) mTOR-mediated phosphorylation of p53 on serine 15 ($p53^{S15}$); (iii) p53-dependent upregulation of the expression of Bax, which undergoes a conformational change and translocates from the cytosol to mitochondria; (iv) Bax-mediated permeabilization of mitochondrial membranes with reduction of the mitochondrial transmembrane potential ($\Delta\Psi_m$) and release of apoptogenic proteins from mitochondria, in particular apoptosis-inducing factor and cytochrome *c*; (v) cytochrome *c*-dependent caspase activation; and (vi) caspase-dependent nuclear chromatin condensation (Ferri *et al*., 2000a; Castedo *et al*., 2001). This sequence of events has been observed in Env-transfected HeLa cells co-cultured with

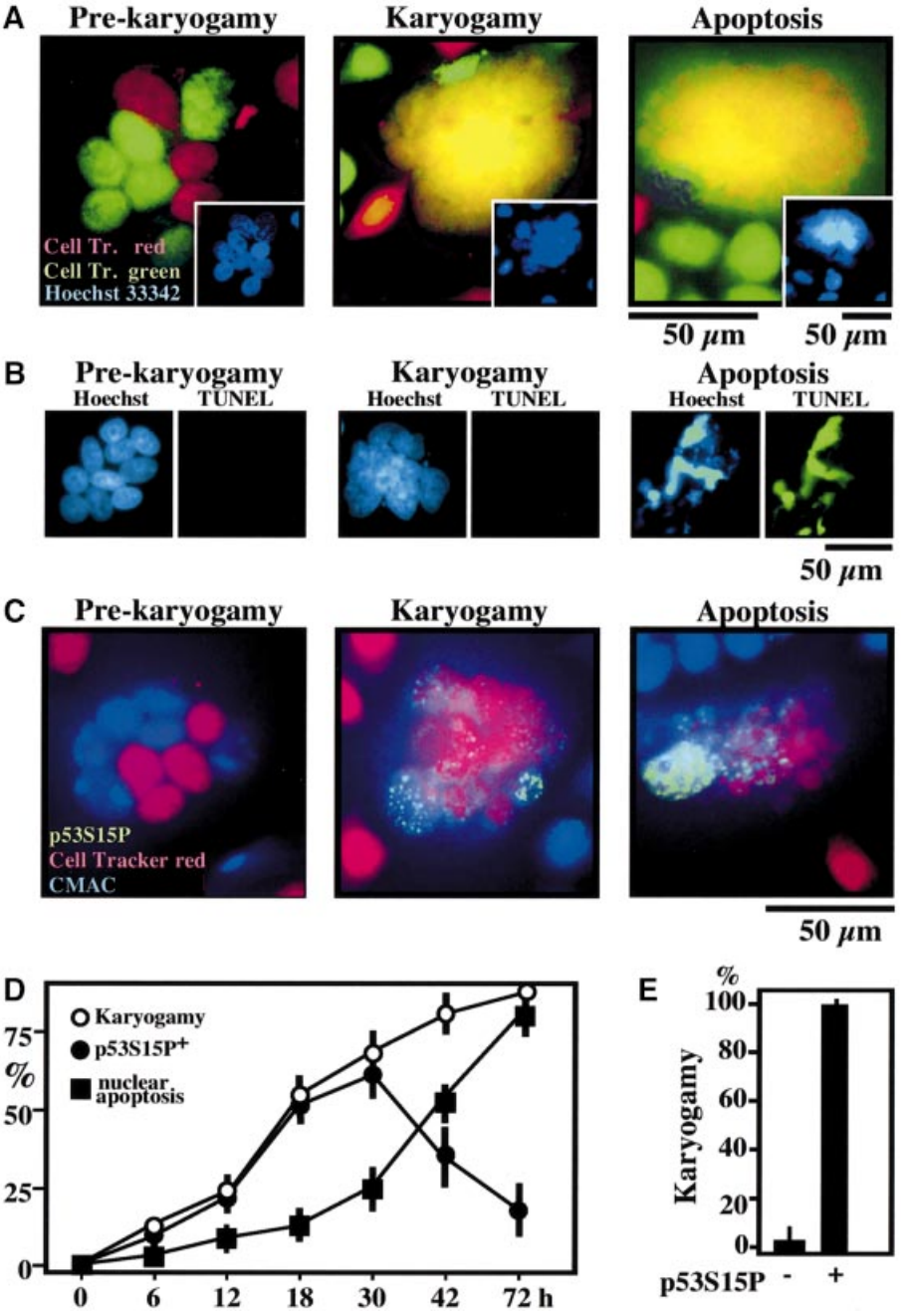

Fig. 1. Karyogamy correlating with p53^{S15} phosphorylation in HIV-1 Env-elicited syncytia. (**A**) Detection of nuclear fusion. HeLa Env and HeLa CD4 cells were stained with CellTracker Red and Green, respectively, followed by co-culture for 18 h. Representative fluorescence micrographs of Hoechst 33342-counterstained syncytia exhibiting cytoplasmic fusion without nuclear fusion ('pre-karyogamy'), nuclear fusion without apoptosis ('karyogamy') and nuclear fusion with apoptosis are shown. Note that karyogamy correlates with a Hoechst 33342-detectable loss of internuclear boundaries (inserts). (**B**) DNA degradation assessed by TUNEL staining is restricted to cells exhibiting apoptotic chromatin condensation. (**C**) Coincidence of karyogamy and p53^{S15}P phosphorylation. HeLa Env and HeLa CD4 cells were pre-stained with CellTracker Red or CMAC, respectively, then fused by co-culture, fixed, permeabilized and stained for p53^{S15}P. Representative images are shown, showing that karyogamic cells lacking signs of apoptosis are p53^{S15}P^{+}. (**D**) Kinetics of karyogamy, p53^{S15} phosphorylation, and nuclear apoptosis [detected as in (C)]. (**E**) Quantitation of karyogamy among syncytia as a function of the phosphorylation status of p53^{S15}, 18 h after co-culture. At this stage, p53^{S15}P can be considered as a surrogate marker of karyogamy.

CD4-transfected HeLa cells, in the absence of viral infection (Ferri *et al*., 2000a; Castedo *et al*., 2001), and has been confirmed for HIV-1-infected primary CD4^{+} lymphoblasts (Ferri *et al*., 2000a; Castedo *et al*., 2001; Genini *et al*., 2001; Petit *et al*., 2002).

Intrigued by these premises, we employed a combination of proteomics and hypothesis-driven research with the aim of dissecting the molecular events occurring immediately upstream of mTOR activation. Recently, we discovered that the Env–CD4 interaction not only causes fusion of the cytoplasm but results, after a lag phase, in fusion of the nucleoplasm (karyogamy) (Ferri *et al*., 2000b). Here, we report that Env-elicited nuclear fusion results from the abortive initiation of mitosis, involving the transient activation of cyclin B-dependent kinase-1 (Cdk1). Importantly, our results reveal the existence of a

novel, pro-apoptotic signal transduction pathway elicited by HIV-1, both *in vivo*, in HIV-1-infected patients, and *in vitro*, in HIV-1-infected lymphoblasts. This lethal pathway involves the sequential action of Cdk1, mTOR and p53.

Results and discussion

p53^{S15} phosphorylation correlates with karyogamy in syncytia elicited by HIV-1 Env

HeLa cells stably transfected with a lymphotropic HIV-1 *Env* gene (HeLa Env) were fused by co-culture with CD4/CXCR4-expressing HeLa cells (HeLa CD4). Fusion events, which depend on the Env–CD4 interaction (Ferri *et al*., 2000a,b,c; Castedo *et al*., 2001), were monitored by means of two stable, non-toxic CellTracker fluorescent dyes with which HeLa Env (CellTracker Green) or HeLa CD4 cells (CellTracker Red) were pre-incubated. After several hours of co-culture, juxtaposed nuclei from both cell types (red or green) could be distinguished within a common cytoplasm (Figure 1A). Subsequently, nucleoplasm fusion (karyogamy) occurred, as detectable by the blending of the two CellTracker dyes (yellow) within the nucleus. Twenty-four hours post-fusion ~50% of syncytia induced by the Env–CD4 interaction exhibited karyogamy, and this percentage was <10% for syncytia arising from PEG-mediated cellular fusion (data not shown). Karyogamy induced by the Env–CD4/CXCR4 interaction occurred before apoptotic nuclear chromatin condensation (detected with Hoechst 33342, Figure 1A) and DNA degradation (detected by TUNEL staining, Figure 1B). Apoptosis, in turn, was only found in karyogamic syncytia (Figure 1A and B). Similar results were obtained when the two fusion partners were labeled with CellTracker Red and CMAC (blue fluorescence, Figure 1C). Karyogamy (as defined by the purple blend of red and blue fluorescence) correlated with p53^{S15} phosphorylation (revealed in green), as indicated by triple staining experiments (Figure 1C and E) and kinetic analyses (Figure 1D). These data suggest that illicit nuclear fusion, linked to p53^{S15} phosphorylation, may be involved in syncytial apoptosis.

Karyogamy results from an abortive entry into the mitotic prophase

Quantitative immunoblots performed with a panel of ~900 monoclonal antibodies revealed that a cluster of proteins accumulating at the G_2/M boundary were overexpressed in HIV-1 Env-elicited syncytia, early after fusion, at 9 h (Figure 2A). This applies to AIM1 (aurora- and Ip1-like midbody-associated protein), IAK1 (IP1- and aurora-related kinase-1), PLK-1 (polo-like kinase-1), the serine-threonine kinase Nek2 and the topoisomerase IIα isoform and its binding protein (ToBP1). Among the cyclins, only cyclin B was altered, with a transient overexpression at 18 h (Figure 2A and B). Based on this information, we determined the relationship between karyogamy and cell cycle. Whereas individual nuclei from pre-karyogamic syncytia incorporated the DNA precursor BrdU, no signs of DNA synthesis could be detected in karyogamic nuclei (Figure 2C). Karyogamic nuclei stained for tubulin (Figure 2D) and exhibited a loss in lamin B staining, indicating the dissolution of the nuclear envelope (Figure 2E). Accordingly, a dextran–FITC conjugate (molecular weight 70 kDa) microinjected into the cytoplasm was excluded from nuclei of pre-karyogamic syncytia, yet did penetrate into karyogamic nuclei (Figure 2F). These features (arrest of DNA synthesis and annihilation of the barrier function of the nuclear envelope) suggest that karyogamy corresponds to the entry into the early mitotic prophase, before spindle formation and pronounced mitotic chromatin condensation occur. Cyclin B was found to accumulate in the cytosol (and sometimes in the nucleus) of syncytia before karyogamy, yet was absent from most karyogamic cells, with a peak increase ~12 h after Env–CD4 co-cultures (Figure 2G). This suggests that the Cdk1, which is required for lamin phosphorylation/depolymerization and progression through mitosis (Smits and Medema, 2001), has been inactivated early after karyogamy. Accordingly, the inactivating phosphorylation of Cdk1 on Tyr15 (Kumagai and Dunphy, 1991) was found to be a relatively late event (Figure 2H). Immunoprecipitation of the cyclin B–Cdk1 complex confirmed a higher Cdk1 activity (measured on histone H1) in syncytia as compared with individual control cells, and this increase in kinase activity peaked at ~12 h (Figure 2I).

Cdk1 is involved in karyogamy and syncytial apoptosis

Addition of Cdk1 inhibitor roscovitine to HeLa Env/HeLa CD4 co-cultures prevented karyogamy, as well as p53^{S15} phosphorylation and all subsequent steps leading to apoptosis such as mitochondrial translocation of Bax, loss of the $\Delta\Psi_m$ and apoptotic chromatin condensation (Figure 3A and B). Roscovitine allowed for the formation of larger syncytia, with more nuclei (Figure 3C). Roscovitine failed to inhibit apoptosis induced by

Fig. 2. Phenotypic characterization of Env-induced karyogamy. (**A**) Cell cycle-relevant proteins whose expression level changes (by a factor of ⩾2) upon syncytium formation as determined by quantitative immunoblots (X ± SEM, n = 3). (**B**) Examples of cell cycle-relevant proteins detectable in HeLa cells whose expression level varies by a factor <2. (**C**) 5-bromo-2′deoxyuridine (BrdU) incorporation into syncytia as a function of the karyogamy (KG) status. Sixteen-hour-old syncytia were incubated with BrdU for 2 h and then subjected to the immunodetection of BrdU into S-phase nuclei. (**D**) Tubulin staining of 18-h-old syncytia. Note that the tubulin network is excluded from the nucleus before karyogamy. After karyogamy, nuclei stain positively for tubulin. (**E**) Lamin B immunostaining of syncytia. Note that karyogamic syncytia exhibit the breakdown of lamin B. (**F**) Loss of nuclear envelope barrier function in karyogamy. Syncytia were microinjected into the cytoplasm with dextran-70 FITC conjugated, which is excluded from the nucleus of pre-karyogamic cells, yet penetrates into the nucleus of karyogamic syncytia. (**G**) Cyclin B accumulation in pre-karyogamic syncytia. Two phenotypes (12 h after fusion) are shown, namely pre-karyogamic (p53^{S15}P$^+$) cells exhibiting cyclin B in the cytoplasm or in the nucleus. In contrast, most karyogamic cells lack immunodetectable cyclin B. The kinetics of cyclin B accumulation is shown at different intervals. The few karyogamic (p53^{S15}P$^+$) cells positively staining for cyclin B demonstrate a diffuse (cytoplasmic + nuclear) staining pattern. (**H**) Kinetics of cyclin B accumulation and the phosphorylation of p53^{S15} or Cdk1T15. (**I**) Kinetics of Cdk1 activity. Cdk1 was immunoprecipitated at different intervals after syncytium formation and its capacity to phosphorylate histone H1 *in vitro* was determined (H1-P*) in the absence or presence of roscovitine (1 μM). Immunoblot detection to confirm equal loading of Cdk1 was also performed.

staurosporine or by HIV-1-encoded viral protein R (Vpr), indicating that it does not act as a general apoptosis inhibitor (such as Bcl-2; Figure 3D). Chemically unrelated Cdk1 inhibitors such as purvalanol, olomoucine and *N*-9 isopropyl-olomoucine inhibited the Env-elicited $p53^{S15}$ phosphorylation and apoptosis, much as roscovitine did (Figure 3E). These pharmacological data were corroborated at the genetic level, by transient transfection with a dominant-negative (DN) cyclin Cdk1 mutant (Figure 3F), which prevented karyogamy, $p53^{S15}$ phosphorylation and

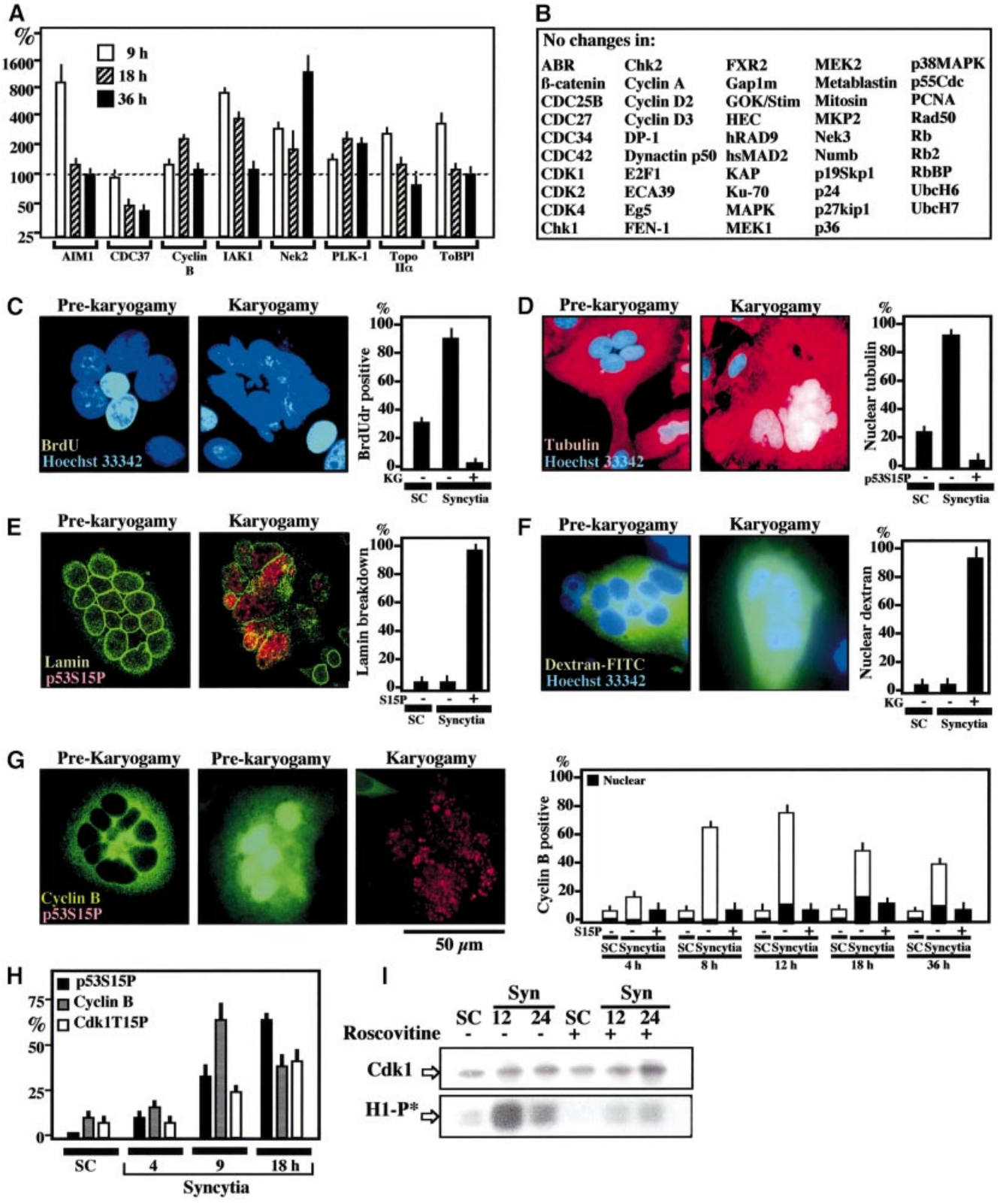

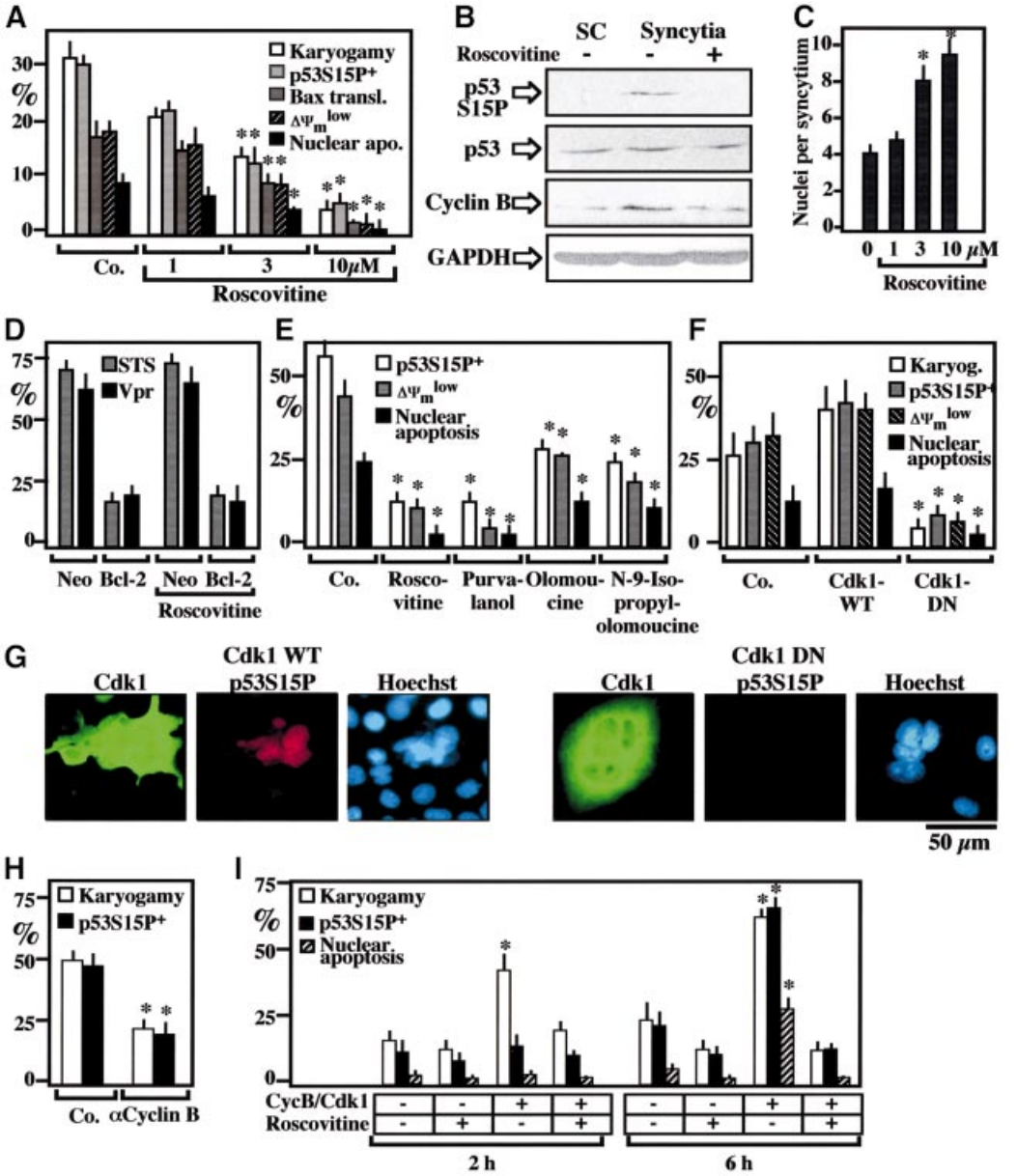

Fig. 3. Involvement of Cdk1 in karyogamy and apoptosis. (**A**) Effects of the Cdk1 inhibitor roscovitine on karyogamy, p53^{S15} phosphorylation, Bax upregulation and signs of apoptosis. Values (X ± SEM, n = 3), obtained after 16 h of co-culture, are representative of seven independent experiments. Asterisks denote significant (P < 0.01, Student's t-test) differences compared to untreated control cultures. (**B**) Roscovitine (10 μM)-mediated inhibition of p53^{S15} phosphorylation, as determined by immunoblot detection. A 1:1 mixture of HeLa CD4/HeLa Env single cells (SC) or syncytia (18 h of co-culture) generated in the absence or presence of 10 μM roscovitine were subjected to immunoblotting analysis. GAPDH was detected to confirm equal protein loading (40 μg per lane). (**C**) Roscovitine-mediated increase in the syncytial size (determined by counting the number of Hoechst 33342-stained nuclei per syncytium, n = 100). (**D**) Failure of roscovitine to act as a general apoptosis inhibitor. HeLa cells stably transfected with Bcl-2 or the Neo resistance gene only were exposed for 6 h to 4 μM staurosporine (STS) or synthetic Vpr peptide, followed by the cytofluorometric assessment of the frequency of cells incorporating the vital dye propidium iodide (X ± SEM, n = 3). (**E**) Comparative assessment of different pharmacological Cdk1 inhibitors. HeLa Env/HeLa CD4 syncytia were generated in the presence of 10 μM roscovitine, 3 μM purvalanol, 60 μM olomoucine or 30 μM *N*-9-isopropylolomoucine, and the indicated parameters were scored 24 h after initiation of co-cultures. (**F**) Effect of DN Cdk1 on p53^{S15} phosphorylation, apoptosis and syncytial size. Cells were transiently transfected 24 h before fusion with vector only (Co.), wild-type (WT) or DN Cdk1 and the indicated parameters were determined 16 h after co-culture among cells strongly staining for Cdk1-WT or Cdk1-DN. (**G**) Representative immunostainings of syncytia transfected with either Cdk1-WT or Cdk1-DN [as in (F)] and stained with antibodies specific for Cdk1 (which also recognizes Cdk1-DN) and p53^{S15}P. (**H**) Microinjection of a neutralizing cyclin B antibody into newly formed syncytia. A cyclin B-specific monoclonal antibody (or an anti-paxillin antibody serving as a negative control) were microinjected into the cytoplasm of 6-h-old syncytia, and the frequency of karyogamy or p53^{S15} phosphorylation was scored 12 h later. (**I**) Karyogamy triggered by microinjection of cyclin B–Cdk1. Six-hour-old syncytia were microinjected with an active cyclin B–Cdk1 complex or PBS (Co.) and cultured either in the absence or in the presence of 10 μM roscovitine for the indicated period, followed by determination of karyogamy, p53^{S15}P and nuclear apoptosis.

apoptosis (Figure 3F and G). Moreover, microinjection of an anti-cyclin B antibody into 6-h-old syncytia inhibited karyogamy and p53^{S15} phosphorylation (Figure 3H). Injection of an active Cdk1–cyclin B complex into the cytoplasm of freshly formed syncytia resulted into accelerated nuclear fusion, and this effect was prevented

by roscovitine (Figure 3I). This suggests that lamin phosphorylation/depolymerization induced by Cdk1 (Peter *et al*., 1990) is sufficient to induce karyogamy. Microinjection of Cdk1–cyclin B into syncytia also induced karyogamy and, after a lag phase, phosphorylation of $p53^{S15}$ and apoptosis (Figure 3I).

mTOR is activated downstream of Cdk1

One $p53^{S15}$ kinase activated by HIV-1 infection has been identified as mTOR (Castedo *et al*., 2001). Accordingly, mTOR, which is normally found in the cytoplasm of individual HeLa cells, was detected in nuclei from karyogamic ($p53^{S15}$ phosphorylation^{+}) syncytia (Figure 4A). Cdk1 inhibition by roscovitine, which inhibits $p53^{S15}$ phosphorylation and karyogamy (Figure 3A and B), completely suppressed the nuclear relocalization of mTOR, which stayed cytoplasmic (Figure 4A). A similar inhibition of the nuclear localization of mTOR was observed upon transfection with DN-CDK1 or treatment with olomoucine (data not shown). In view of the reported intimate relationship between mTOR and cell size control (Zhang *et al*., 2000; Bodine *et al*., 2001), we tested whether external constraint on cell size of HeLa Env/HeLa CD4 heterokarya would modulate syncytial apoptosis via an effect on the subcellular localization and activity of mTOR. Syncytia cultured on adhesive squares of 20 μm diameter (Ferri *et al*., 2000c) exhibited a reduced number of nuclei per syncytium (2.9 ± 0.3 versus 4.7 ± 1.2 on unpatterned control substrates, 18 h after co-culture, X ± SEM, $n = 100$, $P < 0.001$), as well as increased Bax translocation and apoptosis (Figure 4B). However, the reduction of syncytial size had no effect on cyclin B accumulation, karyogamy, nuclear accumulation of mTOR and $p53^{S15}$ phosphorylation (Figure 4B). Culture on a substrate specifically designed to increase spreading via extension of cell processes that attach to squares of 5 μm in diameter, separated by 10 μm of non-adhesive zones [5/10 self-assembled monolayer (SAM)] (Figure 4B) (Chen *et al*., 1997; Ferri *et al*., 2000c) resulted in an increase in the average number of nuclei per syncytium (7.2 ± 2.8, $P < 0.001$). In spite of the inhibition of Bax translocation and apoptosis by the 5/10 SAM, there was no effect on the nuclear relocalization of mTOR (Figure 4B). Taken together, these data suggest that, downstream of cyclin B, mTOR is activated by a pathway that is not linked to cell size control.

mTOR mediates $p53^{S15}$ phosphorylation downstream of Cdk1

mTOR inhibition by rapamycin reduced $p53^{S15}$ phosphorylation, as well as all downstream events leading to cell death including Bax translocation, $\Delta\Psi_m$ dissipation and nuclear condensation (Figure 4C). Rapamycin had no effect on the accumulation of cyclin B preceding karyogamy. Unexpectedly, however, rapamycin reduced karyogamy in HeLa Env/HeLa CD4 heterokarya (Figure 4C), an observation that is reminiscent of that obtained in *Saccharomyces cerevisiae*, in which rapamycin can inhibit karyogamy (Choi *et al*., 2000). While these data indicate that both Cdk1 and mTOR engage in an intricate pathway regulating nuclear fusion, they do not prove that mTOR is directly phosphorylating $p53^{S15}$. We therefore transfected individual HeLa cells with mTOR.

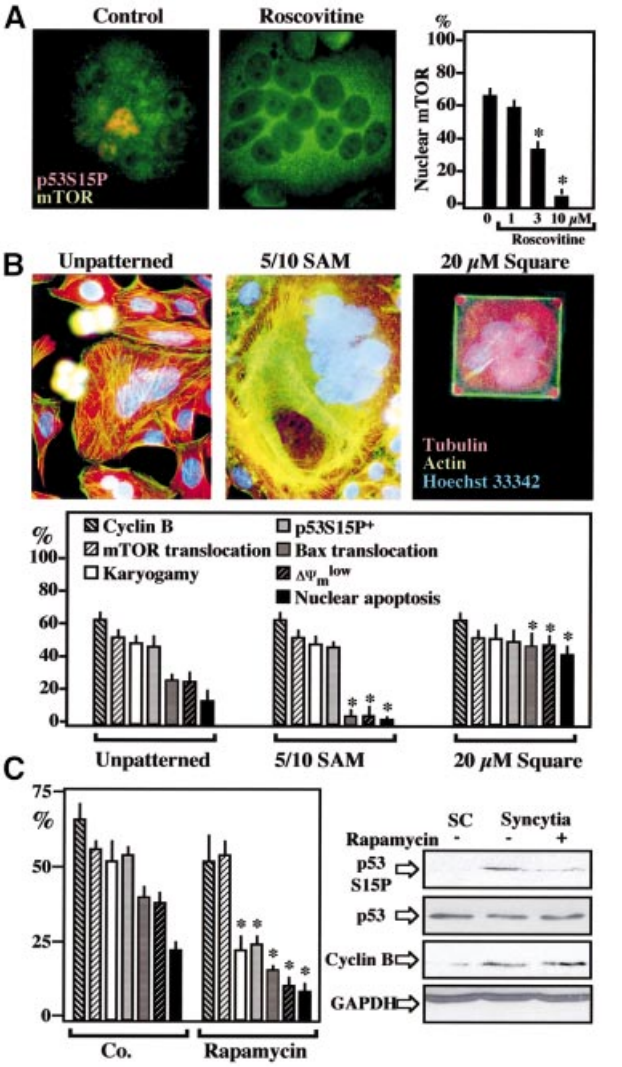

Fig. 4. mTOR involvement in karyogamy and $p53^{S15}$ phosphorylation. (**A**) mTOR acts downstream of Cdk1. Untreated 24-h-old syncytia (Co.) or syncytia cultured in the continuous presence of roscovitine were subjected to immunodetection of mTOR. Note that roscovitine prevents the nuclear accumulation of mTOR as well as $p53^{S15}$ phosphorylation. (**B**) Failure of cell size to modulate karyogamy or mTOR. Syncytia were generated on unpatterned substrates or on specialized culture substrates designed to increase cellular spreading and syncytial size (5/10 SAM) or to exert an external constraint on cell size (square-shaped SAM 20 μM in diameter). Representative staining patterns of actin and tubulin networks are shown. Note the actin stress fibers in the 5/10 SAM syncytia and the rigorously square-shaped cell cultured on the 20-μm square SAM. Twenty-four hours after co-culture, the frequency of cells exhibiting cyclin B upregulation, karyogamy, $p53^{S15}P$ phosphorylation, nuclear relocalization of mTOR or apoptotic parameters were determined. Asterisks indicate significant differences ($P < 0.01$) as compared with unpatterned control substrates. (**C**) Effect of rapamycin on syncytia. HeLa CD4 and HeLa Env cells were co-cultured in the absence (Co.) or presence of the mTOR inhibitor rapamycin (1 μM), followed by determination of the indicated parameters at 30 h, either by *in situ* fluorescence techniques (columns) or by immunoblot. The color coding is as in (B). Asterisks denote significant ($P < 0.01$) effects.

Most cells that overexpress mTOR exhibited $p53^{S15}$ phosphorylation (Figure 5A). mTOR immunoprecipitated with an anti-Flag antibody from a cell line stably transfected with flagged mTOR (but not that of a kinase-

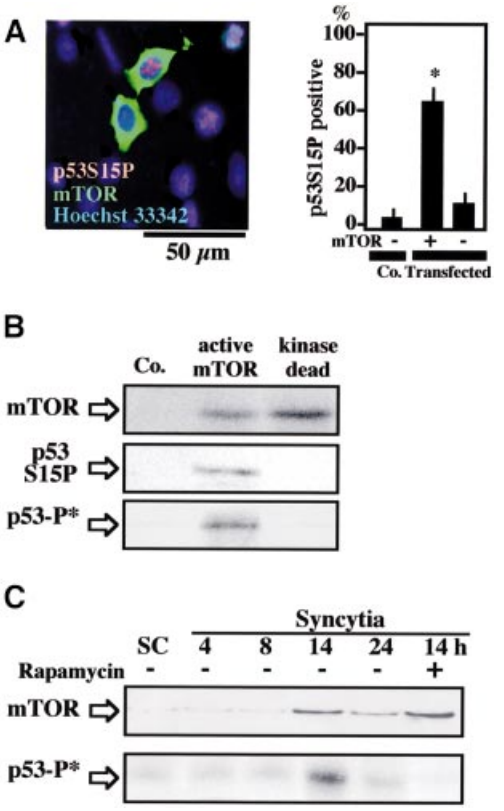

Fig. 5. mTOR-mediated p53^{S15} phosphorylation. (**A**) Overexpression of mTOR is sufficient to cause p53^{S15} phosphorylation. Wild-type HeLa cells were transfected with mTOR, and the frequency of p53^{S15}P^{+} cells among mTOR-overexpressing cells and vector-only transfected (Co.) cells was detected by two-color immunofluorescence staining. Asterisks denote significant ($P < 0.01$) effects as compared with controls. (**B**) *In vitro* phosphorylation of recombinant p53 by recombinant mTOR. mTOR was immunoprecipitated from untransfected HEK293 cells (Co.) or HEK293 cells stably transfected with active or kinase-dead FLAG-mTOR, using an anti-FLAG antibody, and assayed for its capacity to phosphorylate recombinant p53 *in vitro*, in the presence of [γ-^{32}P]ATP, either by autoradiography (p53-P*) or by immunoblot with an antibody specific for p53^{S15}P. (**C**) *In vitro* phosphorylation of recombinant p53 by mTOR expressed in syncytia. mTOR was immunoprecipitated from freshly mixed HeLa CD4 and HeLa Env cells (single cells, SC) or from co-cultures, using an mTOR-specific antibody, and its capactity to phosphorylate p53 was assessed *in vitro* as in (B), in the absence or presence of 1 μM rapamycin (added during cell culture as well as *in vitro*).

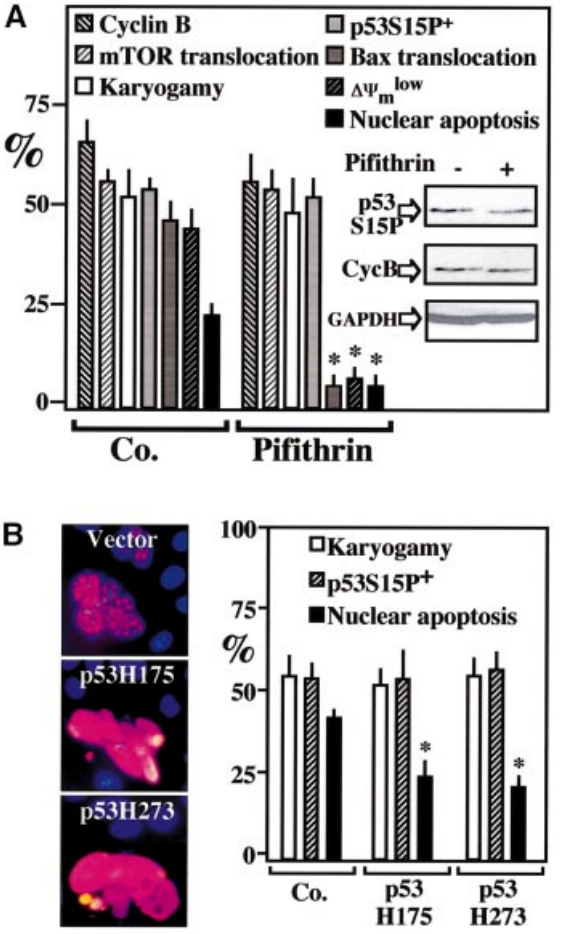

Fig. 6. p53 phosphorylation occurs downstream of cyclin B/mTOR upregulation and karyogamy. (**A**) Chemical inhibition of p53 by cyclic pifithrin-α. Syncytia were generated in the presence of 10 μM cyclic pifithrin-α, and the indicated parameters were determined by *in situ* fluorescence techniques (columns) or by immunoblotting (insert). Asterisks denote significant ($P < 0.01$) pifithrin-α effects. (**B**) Effect of DN p53. Syncytia were generated by co-culture of HeLa CD4 and HeLa Env cells previously transfected with either of two p53 mutants. Note that the level of p53^{S15}P staining, at per-cell level, actually increased and that karyogamy and the frequency of p53^{S15}P^{+} cells was not affected, while apoptosis was inhibited corresponding to the transfection efficiency (~50%). Results are representative of three independent determinations.

dead mTOR mutant) (Fang *et al*., 2001) phosphorylated recombinant p53 *in vitro* (Figure 5B). Endogenous mTOR immunoprecipitated from HeLa Env–CD4 syncytia exhibited a higher capacity to phosphorylate p53 *in vitro* than mTOR from individual cells, correlating with enhanced mTOR expression levels (Figure 5C). When added to HeLa Env–CD4 syncytia, the p53 inhibitor pifithrin-α (Komarov *et al*., 1999) had no effect on cyclin B accumulation, karyogamy or p53^{S15} phosphorylation, yet did prevent the mitochondrial and nuclear signs of apoptosis (Figure 6A). Similar results were obtained by transfection with DN p53 mutants, which had no effect on karyogamy nor on p53^{S15} phosphorylation, yet prevented apoptosis (Figure 6B). Thus, p53 operates downstream from the Cdk1/mTOR-controlled karyogamy step leading to syncytial apoptosis.

mTOR and p53^{S15} phosphorylation in lymph nodes and peripheral blood mononuclear cells from HIV-1 patients

Phosphorylated p53^{S15} could be detected in single cells as well as in syncytia localized in the T cell area of lymph nodes from HIV-1^{+} patients. The same syncytia overexpress mTOR, as revealed by immunostaining of adjacent sections (Figure 7A). p53^{S15} phosphorylation was detected in peripheral blood mononuclear cells (PBMC) of HIV-1^{+} donors but not in PBMC from HIV-1^{-} controls (<1% positive cells), correlating with the frequency of mTOR-overexpressing PBMC (Figure 7B). Such p53^{S15}P^{+} or mTOR^{+} cells were found among all relevant PBMC populations (CD4^{+}, CD8^{+}, CD14^{+}), with a preference for monocytes (CD14^{+}) (Figure 7C). In accordance with the previous finding establishing a positive correlation

between viral load and the frequency of $p53^{S15}P^+$ PBMC in HIV-1^+ carriers (Castedo *et al*., 2001), untreated HIV-1^+ donors exhibited far higher levels of $p53^{S15}P^+$ and $mTOR^+$ cells than patients in which the number of viral copies had dropped as a result of ongoing highly active anti-retroviral therapy (HAART). This difference persisted among patients that continued to have low levels of circulating HIV-1 particles after HAART interruption (Figure 7D). In conjunction with the previously reported finding that cyclin B is overexpressed in PBMC from HIV-1 patients (Cannovo *et al*., 2001), these data underline the probable *in vivo* relevance of the HIV-1-induced lethal Cdk1/mTOR/p53 pathway.

Cdk1 is critically involved in syncytial cell death induced by HIV-1 infection

Primary $CD4^+$ lymphoblasts from healthy donors were infected with the lymphotropic $HIV\text{-}1^{IIIb}$ strain *in vitro*, a manipulation that induces syncytium formation and subsequent apoptosis. According to one report (Wang *et al*., 2001), Cdk1 inhibition by roscovitine may affect HIV-1 transcription. However, addition of non-toxic doses ($\leqslant 1$ μM) of roscovitine 48 h after infection failed to inhibit viral replication, as determined by quantifying the production of p24 (Figure 8). Moreover, roscovitine did not reduce the HIV-1-triggered syncytium formation and rather led to the formation of giant syncytia, occasionally containing >100 nuclei (Figure 8B). Roscovitine did inhibit chromatin condensation, as well as the $\Delta\Psi_m$ loss in HIV-1-elicited syncytia (indicated by a red–green shift in the fluorescence of JC-1-stained cells). Similar results were obtained when roscovitine was replaced by another Cdk1 inhibitor, olomoucine (Figure 8B and C). This inhibition was similar to that obtained by rapamycin (Castedo *et al*., 2001; data not shown). Altogether, these data confirm that the roscovitine/olomoucine-inhibited CDK1→mTOR→$p53^{S15}P$ pathway selectively controls apoptosis of syncytia in human primary $CD4^+$ lymphocytes infected by HIV-1.

Conclusions

Syncytia elicited by HIV-1 Env progress to apoptosis in a stepwise fashion. After an initial stage ('stage I'; Figure 9), during which nuclei are separated by intact envelopes, cyclin B accumulates in the cytoplasm, mTOR remains a predominantly cytoplasmic protein and $p53^{S15}$ is non-phosphorylated. Later, syncytia adopt a different phenotype ('stage II'; Figure 9), with nuclear fusion (karyogamy), dismantled nuclear envelopes, downregulated cyclin B, mTOR in the nucleus and $p53^{S15}$ phosphorylation (Figures 1 and 2). Altogether, these changes resemble 'mitotic catastrophe' (Pines, 1999), an apoptosis-like process that begins in prophase, after dissolution of the nuclear membrane, and is associated with the entry of Cdk1 and cyclin B into the nucleus, which can be found in a minority of stage I cells (Figure 2G). Molecular ordering of the process has been achieved using a battery of chemical inhibitors (of Cdk1, mTOR, p53), DN constructs (of Cdk1 and p53) and positive manipulations (microinjection of Cdk1–cyclin B, transfection with mTOR) (Figures 3–8). Upon syncytium formation, cyclin B is upregulated in a transient fashion, thereby triggering Cdk1-dependent activation of lamin disassembly (which facilitates karyogamy) and nuclear accumulation of mTOR. mTOR, which contributes to karyogamy, then phosphorylates $p53^{S15}$, resulting in the transcriptional activation of apoptogenic p53 target genes (Figure 9). That mTOR (or a closely associated kinase) directly phosphorylates p53 is suggested by the facts that mTOR co-immunoprecipitates with p53 in syncytia but not in normal cells (data not shown), that mTOR translocates to the nuclei (Figure 4A) and that immunoprecipitated mTOR from mTOR-transfected normal cells or from syncytia can phosphorylate recombinant p53 *in vitro* (Figure 5). Intriguingly, physiological syncytia (myotubes, osteoclasts, syncytiotrophoblasts) can only form after differentiation-associated irreversible cell cycle arrest, and do not

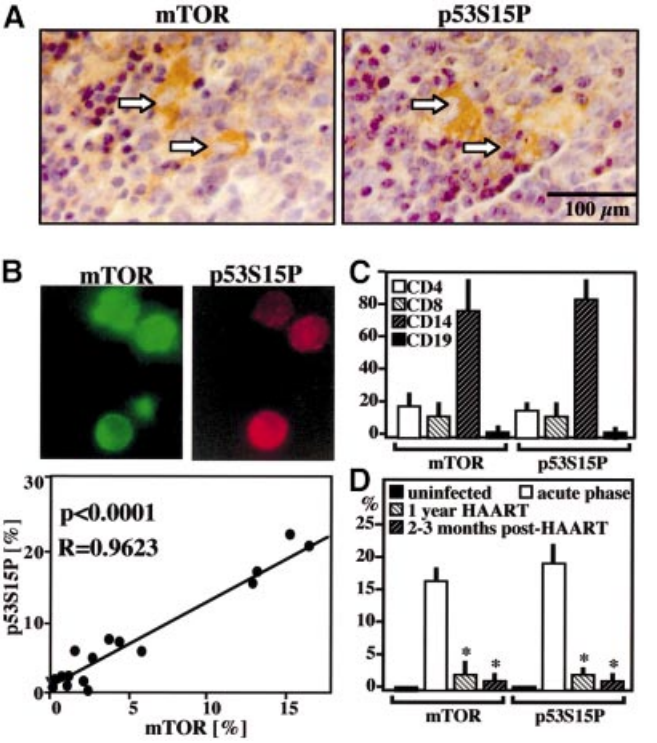

Fig. 7. Detection of mTOR and $p53^{S15}P$ in HIV-1 patients. (**A**) Immunocytochemical localization of $p53^{S15}P$ and mTOR in lymph node biopsies from HIV-1^+ patients. Two adjacent sections are shown. Arrows indicate positive stainings, which are virtually absent in lymph node from uninfected controls. Similar results were obtained with biopsies from three further untreated HIV-1^+ donors. Less than 0.1% of the cells from normal donors stain positively for $p53^{S15}P$ and mTOR. (**B**) Immunolocalization of $p53^{S15}P$ (red fluorescence) and mTOR (green fluorescence) proteins in PBMC from HIV-1^+ patients. Note that most cells are positive for both markers. The frequency of $mTOR^+$ and $p53^{S15}P^+$ was determined among total PBMC of 21 HIV-1^+ patients. Each dot represents one patient. Calculations were done following the Pearson method. (**C**) Frequency of $mTOR^+$ and $p53^{S15}P^+$ cells among defined subsets of mononuclear cells. A subset of the patients shown in (B) was subjected to two color immunofluorescence stainings, allowing for the determination of the percentage of cells expressing $mTOR^+$ or $p53^{S15}P^+$ among lymphocytes expressing CD4, CD8 or CD19, as well among $CD14^+$ monocytes. (**D**) Effect of HAART on mTOR and $p53^{S15}P$ expression in PBMC from HIV-1^+ donors. The frequency of $mTOR^+$ and $p53^{S15}P^+$ PBMC was determined in uninfected controls, individuals with acute infection (untreated), patients receiving at least 12 months of HAART, as well as individuals with undetectable virus after several months of HAART interruption. Values are means ± SD. Asterisks indicate a significant reduction of the indicated parameters, as compared with untreated controls.

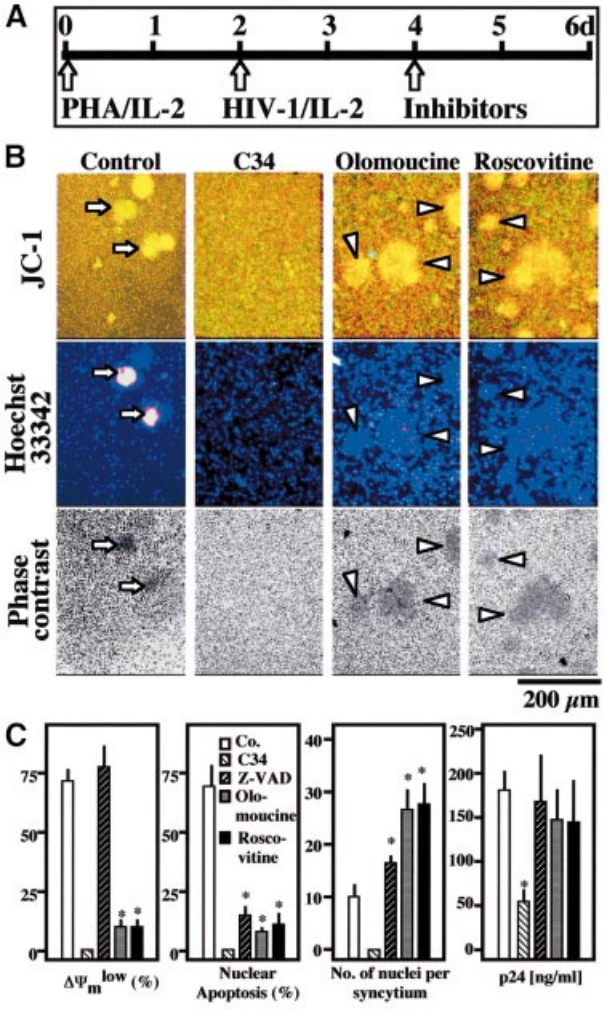

Fig. 8. Involvement of Cdk1 in apoptosis of syncytia induced by HIV-1 infection. (**A**) Experimental set-up. After an initial stage (48 h) stimulation with PHA and interleukin-2 (IL-2), primary CD4$^+$ lymphoblasts were infected with HIV-1^{IIIB}. After 48 h, 1 μM AZT (which blocks viral RNA synthesis), 500 nM C34 (a gp41-derived peptide that blocks Env-mediated fusion), 50 μM Z-VAD.fmk, (a pan-caspase inhibitor) or either of two Cdk1 inhibitors (10 μM olomoucine or 1 μM roscovitine) were added to the cells. After a further 48 h culture period, virological and apoptotic parameters were assessed. (**B**) Representative fluorescence micrographs. Cells were stained with the $\Delta\Psi_m$-sensitive dye JC-1 (red fluorescence indicates a high $\Delta\Psi_m$, green fluorescence a low $\Delta\Psi_m$) and Hoechst 33342 for the detection of chromatin condensation. Arrows indicate apoptotic syncytia, while arrow heads mark syncytia with a high $\Delta\Psi_m$ and no signs of nuclear apoptosis. (**C**) Quantitative determinations. The frequency of cells exhibiting signs of apoptosis, the number of nuclei per syncytium, and production of the viral protein p24 were determined. Note that no syncytia were found in the presence of AZT or C34. Results (mean values ± SEM) are representative of four independent experiments. Asterisks denote significant effects as compared with control cultures ($P < 0.01$).

undergo karyogamy (Bamberger *et al*., 1999; Kitzmann and Fernandez, 2001; Okahashi *et al*., 2001). Thus, maintenance of a post-mitotic status might condition the survival of physiological syncytia, which would contrast with Env-induced syncytia, in which progression to early mitosis automatically triggers cell death.

This scenario, which has been elaborated in co-cultures of two HeLa cell lines expressing either Env or CD4 (Figures 1–6), may be relevant to *in vivo* HIV-1 infection,

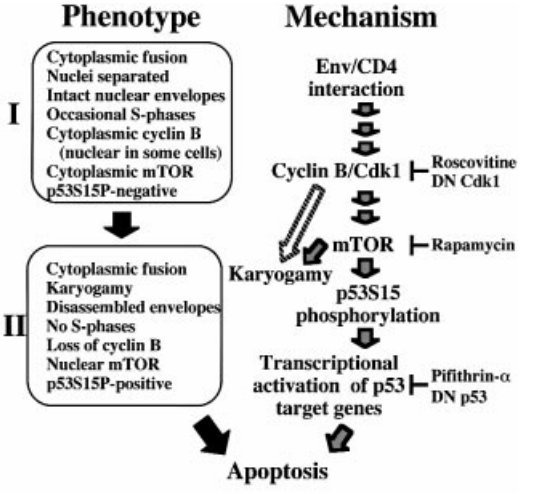

Fig. 9. Mechanisms of Env-triggered apoptosis. After fusion, cells adopt two preponderant phenotypes (stages I and II, left) before they undergo apoptosis, as shown in Figures 1 and 2. The hypothetical molecular order of events (right) is based on the experiments shown in Figures 3–7.

based on several observations. Cyclin B is increased among PBMC from HIV-1-infected patients, a phenomenon that has been attributed to T cell activation (Cannovo *et al*., 2001), but which might also be triggered by the interaction between Env and its (co-)receptors. A significant correlation could be found between mTOR, p53^{S15}P expression, and the virological status of patients (Figure 7). Therapeutic inhibition of HIV-1 replication decreased the expression of cyclin B in PBMC (Cannovo *et al*., 2001) and, as shown here, reduced the frequency of both mTOR$^+$ and p53^{S15}P$^+$ PBMC (Figure 7). Primary CD4 lymphoblasts infected by HIV-1 upregulate cyclin B (Kolesnitchenko *et al*., 1995), and Cdk1 inhibition prevented syncytial cell death induced by HIV-1 infection (Figure 8). Taken together, these data underscore the probable pathophysiological relevance of the novel pro-apoptotic Cdk1–cyclin B→mTOR→p53 pathway delineated in this paper.

Future work will unravel the upstream signal(s) accounting for the HIV-1-stimulated cyclin B–Cdk1 activation, and thus identify the triggers that cause PBMC from HIV-1 carriers to follow a pattern of pro-apoptotic signal transduction which mimics that of Env-elicited syncytia. It remains also an open question through which exact molecular mechanisms Cdk1 activates mTOR, and why Cdk1 activation is transient, leading to an abortive, catastrophic entry into cell cycle. It may be anticipated that the answers to these questions will yield further insights into the pathway by which HIV-1-encoded proteins trigger the devastating apoptosis of immune cells.

Materials and methods

Cell lines, transfection and microinjection

HeLa cells stably transfected with the *Env* gene of HIV-1 LAI (HeLa Env) and HeLa cells transfected with CD4 (HeLa CD4) were cultured alone or together (1:1 ratio), at a density of 1–1.5 × 10^3 cells/mm at the beginning of co-cultures, resulting in progressive cell fusion (with >50% of cells within syncytia within 12 h, when monolayers are near to confluence) (Ferri *et al*., 2000a). Transfection with pcDNA3.1 vector only, wild-type (WT) or DN Cdk1 mutant (van den Heuvel and Harlow,

1993), p53 DN plasmids (gift from T.Soussi), Myc-tagged mTOR/FRAP constructs (Kim and Chen, 2000) was performed by electroporation (Loeffler *et al*., 2001) 24 h before co-culture of HeLa CD4 and HeLa Env cells. HeLa Neo and HeLa Bcl-2 cells (gift from Dr V.Goldmacher) were exposed to staurosporine or synthetic Vpr1-96 peptide (Jacotot *et al*., 2000). In some experiments, all syncytia growing on a pre-marked V-shaped area of a coverslip (>200 per experiment) were microinjected into the cytoplasm (Jacotot *et al*., 2001), with phosphate-buffered saline (PBS) only (pH 7.2), recombinant human cyclin B–Cdk1 (500 U/μl; Promega) (Xie *et al*., 1998), a monoclonal antibody (mAb) specific for cyclin B, or an isotype-(IgG1) matched paxillin mAb (BD Transduction Laboratories) (both at 200 ng/μl). Alternatively, cells were cultured with cyclic pifithrin-α, Cdk1 inhibitors (Calbiochem) or rapamycin (Sigma).

Fluorescence staining of live cells and immunofluorescence

HeLa CD4 cells or HeLa Env cells were labeled with either of three fluorochromes (Molecular Probes) for long-term cell labeling: CellTracker Red, CellTracker Green (15 μM, 30 min at 37°C in complete medium), or CMAC (7-amino-4-chloromethylcoumarin; 15 μM, 30 min in serum-free medium) and washed extensively before co-culture. Live cells were stained with the potentiometric dye 5,5′,6,6′-tetrachloro-1,1′,3,3′-tetraethylbenzimidazolylcarbocyanine iodide (JC-1) and/or Hoechst 33342 (2 μM; Sigma) for 30 min at 37°C (Ferri *et al*., 2000a). A rabbit antiserum specific for p53^{S15}P (Cell Signaling Technology, MA) was used on paraformaldehyde (4% w:v) and picric acid-fixed (0.19% v:v) cells and revealed with a goat anti-rabbit IgG conjugated to phycoerythrine (PE) or FITC (Southern Biotechnology, Birmingham, AL). Cells were also stained for the detection of cyclin B (mAb from BD Transduction Laboratories), lamin B (mAb from Oncogene), Cdk1T15P (Cell Signaling Technology). 5-bromo-2′deoxy-uridine (BrdU) and Tunel staining was performed with detection kits from Roche.

Quantitation of protein expression levels, immunoblots and in vitro kinase assays

Protein samples were prepared from HeLa Env and HeLa CD4 single cells mixed at a 1:1 ratio in lysis buffer (0 control) or from HeLa Env–CD4 syncytia obtained after 9, 18 or 36 h of co-culture. These samples were processed by the PowerBlot facility (Becton Dickinson, Lexington, KY), to measure the expression level of ~900 different signal-transducing proteins using a combination of SDS–PAGE (5–15% gradient), immunoblotting with specific mAbs revealed by a secondary goat anti-mouse horse radish peroxidase, acquisition of chemiluminescence data by a CDD camera, and computerized processing of densitometric data, in triplicate, after normalization on the mean protein expressions. Changes ⩾2 were well above background variations (generally <1.5) observed in these assays (http://www.translab.com/TOC.shtml). Aliquots of protein extracts (40 μg) were subjected to immunoblots using antibodies specific for cyclin B, p53 (BD Transduction Laboratories), p53^{S15}P, or glyceraldehyde-3-phosphated dehydrogenase (GAPDH; mAb from Chemicon). The capacity of immunoprecipitated cyclin B–Cdk1 to phosphorylate histone H1 was assessed (Pines and Hunter, 1994), and a similar protocol was employed to measure the phosphorylation of recombinant p53 (Santa Cruz) by mTOR immunoprecipitated from HeLa cells using an mTOR-specific mAb (Santa Cruz SC8315) or from HEK293 cells stably transfected with pCDNA3-FLAG-mTOR(S2035T) (active mTOR) or pCDNA3-FLAG-mTOR (S2035T, D2357E) (kinase-dead mTOR) lacking the regulatory N-terminus (1362C) (Kim and Chen, 2000; Fang *et al*., 2001).

Preparation of SAMs

An elastomeric stamp with a relief of the predetermined pattern was used to transfer hexadecanethiol (which is compatible with protein absorption) to designated regions of gold-coated glass coverslips. The slides were then immersed in 2 mM tri(ethylene glycol)-terminated alkanethiol (which resists the absorption of proteins) reacting with the bare regions of gold remaining after the printing process (Mrksich *et al*., 1996). Cover slips were pre-coated with human fibronectin (25 μg/ml in PBS, pH 7.2, 2 h at room temperature; Sigma), blocked with bovine serum albumin (10 mg/ml, 20 min at room temperature; Sigma), and rinsed with culture medium containing 1% of fetal calf serum (FCS) before addition of cells (cultured in 1% FCS).

Patients′ samples

Peripheral blood samples were obtained from four healthy and 25 HIV-1-infected individuals (mean age 36 years). Seven patients were naive for HAART with a plasma viral load >100 000 copies/ml; seven patients were HAART-treated with a viral load <5000 copies/ml, and 11 patients were under 2 months of antiretroviral therapy interruption with <50 copies/ml. None of the HIV-1$^+$ patients received interferons, glucocorticoids, was positive for hepatitis B or C, or exhibited signs of autoimmunity. PBMC were fixed with 4% formaldehyde in PBS, pH 7.2. Plasma HIV-1 RNA levels were determined by the bDNA procedure (Versant HIV RNA 3.0) according to the manufacturer's instructions (Bayer). Biopsies of axillary lymph nodes, obtained from healthy donors and HIV-1$^+$ asymptomatic patients, naive for antiretroviral therapy, were fixed with 10% formalin, dehydrated and paraffin embedded. Deparaffinized tissue sections were subjected to immunocytochemistry. Cells were stained with anti-p53^{S15}P (revealed with goat anti-rabbit IgG Alexa Fluor 595) and anti-mTOR (revealed with goat anti-mouse IgG Alexa Fluor 488; Molecular Probes, OR).

HIV-1 infection

Primary CD4$^+$ lymphoblast (10×10^6) cells (Castedo *et al*., 2001) were incubated with the HIV-1^{IIIB} (500 ng of p24) for 4 h at 37°C. After washing out unabsorbed virus, cells (10^6 cells/ml) were cultured in RPMI medium containing 20% FCS and 10 U/ml interleukin-2. Forty-eight hours after infection, when the first syncytia appeared in the infected cultures, Cdk1 inhibitors were added. Viral replication was evaluated by measuring the level of HIV-1 core protein p24 in the supernatant (Innogenetics ELISA kit, Barcelona, Spain).

Acknowledgements

We thank Dr Thierry Soussi (Institut Curie, Paris, France), Dr Sander van den Heuvel (Harvard Medical School, Charlestown, MA) for cDNA constructs, Nathanael Larochette (CNRS, Villejuif, France) for assistance, and the NIH AIDS reagents program (Bethesda, MD) for cell lines. This work has been supported by a special grant from LNC, as well as grants from ANRS, FRM, European Commission (QLG1-CT-1999-00739) (to G.K.) and the Italian Ministery of Public Health (to M.P.).

References

Anderson,J.M. (2000) Multinucleated giant cells. *Curr. Opin. Hematol.*, **7**, 40–47.

Badley,A.D., Pilon,A.A., Landay,A. and Lynch,D.H. (2000) Mechanisms of HIV-associated lymphocyte apoptosis. *Blood*, **96**, 2951–2964.

Bamberger,A., Sudahl,S., Bamberger,C.M., Schulte,H.M. and Loning,T. (1999) Expression patterns of the cell-cycle inhibitor p27 and the cell-cycle promoter cyclin E in the human placenta throughout gestation: implications for the control of proliferation. *Placenta*, **20**, 401–406.

Bateman,A., Bullough,F., Murphy,S., Emiliusen,L., Lavillette,D., Cosset,F.L., Cattaneo,R., Russel,S.J. and Vile,R.G. (2000) Fusogenic membrane glycoproteins as a novel class of genes for the local and immune-mediated control of tumor growth. *Cancer Res.*, **60**, 1492–1497.

Berndt,C., Möpps,B., Angermüller,S., Gierschik,P. and Krammer,P.H. (1998) CXCR4 and CD4 mediate a rapid CD95-independent cell death in CD4+ cells. *Proc. Natl Acad. Sci. USA*, **95**, 12556–12561.

Blaak,H., van't Wout,A.B., Brouwer,M., Hoolbrink,B., Hovenkamp,E. and Schuitemaker,H. (2000) *In vivo* HIV-1 infection of CD45RA$^+$ CD4$^+$ T cells is established primarily by syncytium-inducing variants and correlates with the rate of CD4$^+$ T cell decline. *Proc. Natl Acad. Sci. USA*, **97**, 1269–1274.

Bodine,S.C. *et al*. (2001) Akt/mTOR pathway is a crucial regulator of skeletal hypertrophy and can prevent muscle atrophy *in vivo*. *Nature Cell Biol.*, **3**, 1014–1019.

Cannovo,G. *et al*. (2001) Abnormal intracellular kinetics of cell-cycle-dependent proteins in lymphocytes from patients infected with human immunodeficiency virus: a novel biologic link between immune activation, accelerated T-cell turnover and high levels of apoptosis. *Blood*, **97**, 1756–1764.

Castedo,M. *et al*. (2001) Human immunodeficiency virus 1 envelope glycoprotein complex-induced apoptosis involves mammalian target of rapamycin/FKBP12–rapamycin-associated protein-mediated p53 phosphorylation. *J. Exp. Med.*, **194**, 1097–1110.

Chen,C.S., Mrksich,M., Huang,S., Whitesides,G.M. and Ingber,D.E. (1997) Geometric control of cell life and death. *Science*, **276**, 1425–1428.

Choi,J.H., Adames,N.R., Chan,T.-F., Zng,C., Cooper,J.A. and

Zheng,X.F.S. (2000) TOR signaling regulates microtubule structure and function. *Curr. Biol.*, **10**, 861–864.
Cicala,C., Arthos,J., Rubbert,A., Selig,S., Wildt,K., Cohen,O.J. and Fauci,A.S. (2000) HIV-1 envelope induces activation of caspase-3 and cleavage of focal adhesion kinase in primary human CD4+ T cells. *Proc. Natl Acad. Sci. USA*, **97**, 1178–1183.
Eckert,D.M. and Kim,P.S. (2001) Design of potent inhibitors of HIV-1 entry from the fp41 N-peptide region. *Proc. Natl Acad. Sci. USA*, **98**, 11187–11192.
Fang,Y., Vilella-Bach,M., Bachmann,R., Flanigan,A. and Chen,J. (2001) Phosphatidic acid-mediated mitogenic activation of mTOR signaling. *Science*, **294**, 1942–1945.
Ferri,K.F. *et al*. (2000a) Apoptosis control in syncytia induced by the HIV-1-envelope glycoprotein complex. Role of mitochondria and caspases. *J. Exp. Med.*, **192**, 1081–1092.
Ferri,K.F., Jacotot,E., Geuskens,M. and Kroemer,G. (2000b) Apoptosis and karyogamy in syncytia induced by HIV-1–ENV/CD4 interaction. *Cell Death Differ.*, **7**, 1137–1139.
Ferri,K.F., Jacotot,E., LeDuc,P., Geuskens,M., Ingber,D.E. and Kroemer,G. (2000c) Apoptosis of syncytia induced by HIV-1–Envelope glycoprotein complex. Influence of cell shape and size. *Exp. Cell Sci.*, **261**, 119–126.
Genini,D. *et al*. (2001) HIV induced lymphocyte apoptosis by a p53-initiated, mitochondrion-mediated mechanism. *FASEB J.*, **15**, 5–6.
Gougeon,M.L. and Montagnier,L. (1999) Programmed cell death as a mechanism of CD4 and CD8 T cell depletion in AIDS—Molecular control and effect of highly active anti-retroviral therapy. *Ann. N. Y. Acad. Sci.*, **887**, 199–212.
Jacotot,E. *et al*. (2000) The HIV-1 viral protein R induces apoptosis via a direct effect on the mitochondrial permeability transition pore. *J. Exp. Med.*, **191**, 33–45.
Jacotot,E. *et al*. (2001) Control of mitochondrial membrane permeabilization by adenine nucleotide translocator interacting with HIV-1 Vpr and Bcl-2. *J. Exp. Med.*, **193**, 509–520.
Kim,J.E. and Chen,J. (2000) Cytoplasmic-nuclear shuttling of FKBP12–rapamycin-associated protein is involved in rapamycin-sensitive signaling and translation initiation. *Proc. Natl Acad. Sci. USA*, **97**, 14340–14345.
Kitzmann,M. and Fernandez,A. (2001) Crosstalk between cell cycle regulators and the myogenic factor MyoD in skeletal myoblasts. *Cell. Mol. Life Sci.*, **58**, 571–579.
Kolesnitchenko,V. *et al*. (1995) Human immunodeficiency virus 1 envelope-initiated G_2-phase programmed cell death. *Proc. Natl Acad. Sci. USA*, **92**, 11889–11893.
Komarov,P.G., Komarova,E.A., Kondratov,R.V., Christov-Tselkov,K., Coon,J.S., Chernov,M.V. and Gudkov,A.V. (1999) A chemical inhibitor of p53 that protects mice from the side effects of cancer therapy. *Science*, **285**, 1733–1737.
Kumagai,A. and Dunphy,W.G. (1991) The cdc25 protein controls tyrosine dephosphorylation of the cdc2 protein in a cell-free system. *Cell*, **64**, 903–914.
Lifson,J.D., Reyes,G.R., McGrath,M.S., Stein,B.S. and Engleman,E.G. (1986) AIDS retrovirus-induced cytopathology: giant cell formation and involvement of CD4 antigen. *Science*, **232**, 1123–1127.
Loeffler,M., Daugas,E., Susin,S.A., Zamzami,N., Métivier,D., Nieminen,A.-L., Brothers,G., Penninger,J.M. and Kroemer,G. (2001) Dominant cell death induction by extramitochondrially targeted apoptosis inducing factor. *FASEB J.*, **15**, 758–767.
Maas,J.J., Gange,S.J., Schuitemaker,G., Coutinho,R.A., van Leeuwen,R. and Margolick,J.B. (2000) Strong association between failure of T cell homeostasis and the syncytium-inducing phenotype among HIV-1-infected men in the Amsterdam Cohort Study. *AIDS*, **16**, 1155–1161.
Mohri,H. *et al*. (2001) Increased turnover of T lymphocytes in HIV-1 infection and its reduction by antiretroviral therapy. *J. Exp. Med.*, **194**, 1277–1287.
Mrksich,M., Chen,C.S., Xia,Y., Dike,L., Ingber,D.E. and Whitesides,G.M. (1996) Controlling cell attachment on contoured surfaces with self-assembled monolayers of alkanethiolates on gold. *Proc. Natl Acad. Sci. USA*, **93**, 10775–10778.
Okahashi,N., Murase,Y., Koseki,T., Sato,T., Yamato,K. and Nishihara,T. (2001) Osteoclast differentiation is associated with transient upregulation of cyclin-dependent kinase inhibitors. *J. Cell. Biochem.*, **80**, 339–345.
Peter,M., Nakagawa,J., Doree,M., Labbe,J.C. and Nigg,E.A. (1990) *In vitro* dissassembly of the nuclear lamina and M phase-specific phosphorylation of lamins by cdc2 kinase. *Cell*, **61**, 591–602.
Petit,F., Arnoult,D., Lelievre,J.D., Parseval,L.M., Hance,A.J., Schneider,P., Corbeil,J., Ameisen,J.C. and Estaquier,J. (2002) Productive HIV-1 infection of primary CD4+ T cells induces mitochondrial membrane permeabilization leading to caspase-independent cell death. *J. Biol. Chem.*, **277**, 1477–1487.
Pines,J. (1999) Cell cycle: checkpoint on the nuclear frontier. *Nature*, **397**, 104–105.
Pines,J. and Hunter,T. (1994) The differential localization of human cyclins A and B is due to a cytoplasmic retention signal in cyclin B. *EMBO J.*, **13**, 3772–3781.
Roggero,R., Robert-Hebmann,V., Harrington,S., Roland,J., Verne,L., Jaleco,S., Devaux,C. and Biard-Piechaczyk,M. (2001) Binding of human immunodeficiency virus type 1 gp120 to CXCR4 induces mitochndrial transmembrane depolarization and cytochrome *c*-mediated apoptosis independently of Fas signaling. *J. Virol.*, **75**, 7637–7650.
Sasaki,M., Miyazaki,K., Koga,Y., Kimura,G., Nomoto,K. and Yoshida, H. (2002) Calcineurin-dependent mitochondrial disturbances in calcium-induced apoptosis of human immunodeficiency virus gp160-expressing CD4+ cells. *J. Virol.*, **76**, 416–420.
Scheller,C. and Jassoy,C. (2001) Syncytium formation amplifies apoptotic signals: a new view on apoptosis in HIV infection *in vitro*. *Virology*, **282**, 48–55.
Selliah,N. and Finkel,T.H. (2001) Biochemical mechanisms of HIV induced T cell apoptosis. *Cell Death Differ.*, **8**, 127–136.
Smits,V.A. and Medema,R.H. (2001) Checking out the G_2/M transition. *Biochim. Biophys. Acta*, **1519**, 1–12.
Sodroski,J.G., Goh,W.C., Rosen,A., Campbell,K. and Haseltine,W.A. (1986) Role of the HTLV/LAV envelope in syncytia formation and cytopathicity. *Nature*, **322**, 470–474.
van den Heuvel,S. and Harlow,E. (1993) Distinct roles for cyclin dependent kinases in cell cycle control. *Science*, **262**, 2050–2054.
Vlahakis,S.R., Algeciras-Schimnich,A., Bou,G., Heppelmann,C.J., Villasis-Keever,A., Collman,R.C. and Paya,C.V. (2001) Chemokine-receptor activation by env determines the mechanism of death in HIV-infected and uninfected T lymphocytes. *J. Clin. Invest.*, **107**, 207–215.
Wang,D. *et al*. (2001) Inhibition of human immunodeficienct virus type 1 transcrition by chemic cyclin dependent kinase inhibitors. *J. Virol.*, **75**, 7266–7279.
Xie,Z.H., Schendel,S., Matsuyama,S. and Reed,J.C. (1998) Acidic pH promotes dimerization of Bcl-2 family proteins. *Biochemistry*, **37**, 6410–6418.
Zhang,H., Stallock,J.P., Ng,J.C., Reinhard,C. and Neufeld,T.P. (2000) Regulation of cellular growth by the *Drosophila* target of rapamycin dTOR. *Genes Dev.*, **14**, 2712–2724.

Received February 19, 2002; revised May 29, 2002; accepted June 3, 2002